Stratigraphy and Sedimentology of the Upper Pleistocene to Holocene Lake Chalco Drill Cores (Mexico Basin)

Blas Valero-Garcés, Mona Stockhecke, Socorro Lozano-García, Beatriz Ortega, Margarita Caballero, Peter Fawcett, Josef P. Werne, Erik Brown, Susana Sosa Najera, Kristin Pearthree, David McGee, Alastair G. E. Hodgetts, and Rodrigo Martínez

Abstract The Basin of Mexico is a high elevation (2240 m asl), large (9540 km^2), tectonic endorheic basin developed in the central-eastern Trans-Mexican Volcanic Belt. In 2016, the ICDP MexiDrill project recovered a total of 1152 m of sediments from a maximum depth of 520 m in Lake Chalco, in the SW of the Basin of Mexico. The upper 309.15 m (composite sequence, mc) are composed of fine-grained lacustrine sediments alternating with discrete visible tephra layers, and the lower 200 m are primarily volcaniclastic facies and basaltic lavas with some intercalated fluvial and alluvial facies. Initial lacustrine deposition started in the Chalco Basin, after the deposition of a thick volcaniclastic sequence, and continued until the lake

B. Valero-Garcés (✉)
Instituto Pirenaico de Ecología - Consejo Superior de Investigaciones Científicas (IPE- CSIC), Zaragoza, Spain
e-mail: blas@ipe.csic.es

M. Stockhecke (✉)
Large Lakes Observatory and Department of Earth & Environmental Sciences, University of Minnesota Duluth, Duluth, MN, USA

Eawag, Swiss Federal Institute of Aquatic Science and Technology, Surface Waters – Research and Management, Kastanienbaum, Switzerland
e-mail: mona.stockhecke@eawag.ch

S. Lozano-García · S. S. Najera · R. Martínez
Instituto de Geología, Universidad Nacional Autónoma de Mexico, Ciudad Universitaria, Coyoacán, Mexico

B. Ortega · M. Caballero
Instituto de Geofísica, Universidad Nacional Autónoma de Mexico, Ciudad Universitaria, Coyoacán, Mexico

P. Fawcett · K. Pearthree
Department of Earth & Planetary Sciences, University of New Mexico, Albuquerque, NM, USA

M. R. Rosen et al. (eds.), *Limnogeology: Progress, Challenges and Opportunities*, Syntheses in Limnogeology, https://doi.org/10.1007/978-3-030-66576-0_14

was drained in recent centuries. Lake Chalco has remained as a shallow lake until the present day.

Five main lithotypes throughout the core have been defined: (1) Organic, with (i) organic-rich silty clay, (ii) sapropelic silty clay, and (iii) peat; (2) Diatomaceous, with laminated, banded, and mottled diatomaceous silty clay; (3) Calcareous, with banded or massive carbonate silty clay and ostracod-rich layers; (4) Clastic, with silty clay, sand, and gravel, both clast and matrix-supported; and (5) Volcanic, as (i) volcaniclastic layers (tephras and clastic deposits) and (ii) lavas. Eighteen lithological units have been defined based on lithotypes and magnetic susceptibility values. Laminated diatomaceous facies occurred during phases with deeper depositional environments. Carbonate deposition marked more alkaline, shallower phases. Peat and organic-rich silts deposited during periods with better development of wetlands in the basin. The preliminary chronological framework suggests the lake sequence spans at least the last 367 ky. More saline diatom assemblages in diatomaceous facies and the occurrence of carbonate lithotypes and peat layers suggest relatively lower lake levels during interglacials; higher lake levels during glacial stages are indicated by more frequent freshwater diatom assemblages and the occurrence of finely laminated diatomaceous facies. The detailed stratigraphy and facies descriptions from the MexiDrill cores provide the basis for subsequent development of chronology and paleoenviromental studies of the Mexico basin record. Furthermore, the depositional model for Chalco is applicable to lakes developed in active tectonic and volcanic settings.

Keywords ICDP MexiDrill · Chalco Basin · Mexico Basin · Pleistocene · Holocene · volcanism · lake

Introduction

The pioneering work of Elizabeth Gierlowski and Kerry Kelts in the 1990s produced a global record of lake basins including some Quaternary examples (Gierlowski - Kordesch and Kelts 1994, 2001). During the last decades of the twentieth century and under the umbrella of the International Continental Scientific

J. P. Werne
Department of Geology & Environmental Science, University of Pittsburgh, Pittsburgh, PA, USA

E. Brown
Large Lakes Observatory and Department of Earth & Environmental Sciences, University of Minnesota Duluth, Duluth, MN, USA

D. McGee
Department of Earth, Atmospheric & Planetary Sciences, Massachusetts Institute of Technology, Cambridge, MA, USA

A. G. E. Hodgetts
School of Geography, Earth and Environmental Sciences, University of Birmingham, Edgbaston, Birmingham, UK

Drilling Program (ICDP, https://www.icdp-online.org/home/), a number of long Quaternary lacustrine sequences extending beyond the last glacial cycle have been made available worldwide: Lake Chad (Schuster et al. 2009), Qinghai Lake (Colman et al. 2007; An et al. 2012), Lake Baikal (Lake Baikal Paleoclimate Project Members 1992), Dead Sea (Stein et al. 2011), Bosumtwi (Koeberl et al. 2005), Lake Malawi (Scholz et al. 2007), Potrok Aike (Zolitschka et al. 2013), Lake Van (Litt et al. 2012), El'gygytgyn (Melles et al. 2012), Lake Ohrid (Wagner et al. 2014), and Towuti (Russell et al. 2016) among others. In the Americas, several lacustrine records have provided the basis for detailed reconstructions of the climate and environmental evolution in the tropical regions: e.g., Lake Titicaca (Fritz et al. 2007), Petén Itzá (Hodell et al. 2006), Chalco (Brown et al. 2012), and Junin (Rodbell and Abbott 2012). These long sequences span several glacial cycles and contain a detailed history of the origin and evolution of the lake basins, and provide reconstructions of regional vegetation, climate, and environmental change (Fig. 1a).

In this contribution, we summarize the stratigraphy of Lake Chalco in the Basin of Mexico. Investigations of lake sediments of the Valley of Mexico extend back to the 1950s (see references in Bradbury 1989) and most of the work at Lake Chalco was undertaken by researchers at the Universidad Nacional Autónoma de Mexico (UNAM) since the 1990s (see detailed references in Lozano-Garcia et al. 1993; Lozano-Garcia and Ortega-Guerrero 1994, 1998,; Caballero and Ortega Guerrero 1998; Caballero et al. 1999). These studies focused on relatively short (<25 m) cores spanning the last 40 kyr, utilized sedimentary facies, magnetic mineralogy, pollen, and diatom data and transfer functions to reconstruct paleoenvironmental conditions. They showed broadly that lake salinity was higher prior to 27 ka, decreased

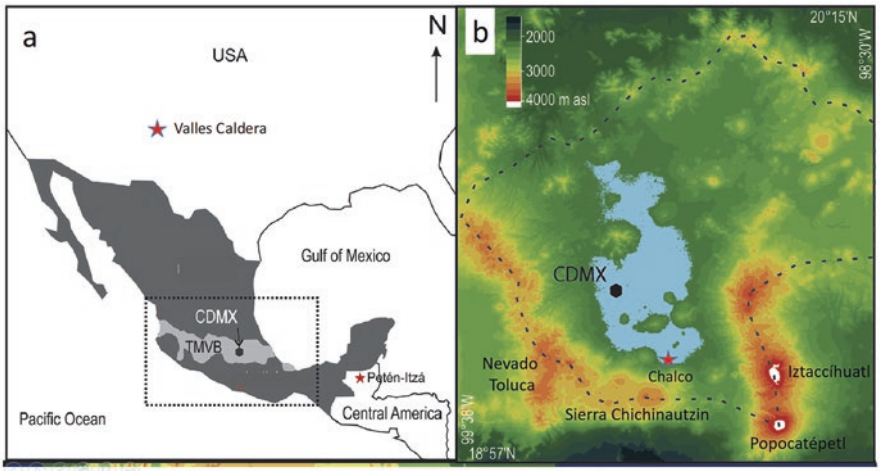

Fig. 1 (**a**) The Trans-Mexican Volcanic Belt (TMVB, light gray area), with the location of Mexico City (CDMX), and some long lacustrine records from the tropics and subtropics of North and Central America (Valles Caldera, New Mexico, USA; Lake Chalco (close to CDMX), Mexico); Petén Itza (Guatemala) (from Caballero et al. 2019). (**b**) Map of the Basin of Mexico showing maximum extent of Lake Chalco during the Pleistocene, Mexico City, and major volcanic centers within the Basin of Mexico and drill site location (red star)

during the Last Glacial Maximum and deglaciation, and increased again during the Early Holocene as temperatures increased. Several drought episodes occurred in Central Mexico during the Late Holocene and, even though human impact limits the interpretation of many records in the region, the late Classic drought (AD 600–1100) seems to have been the most important (Metcalfe et al. 2010). Longer cores from the Chalco Basin recovered in 2008 (>125 m) reached to the last interglacial and show a complex stratigraphy with numerous interbedded volcaniclastic deposits, abundant diatom-rich and laminated facies, and some carbonate-rich intervals (Avendaño 2017; Ortega et al. 2015; Lozano-García et al. 2015). In 2016, the complete lacustrine sequence of the Chalco Basin (>500 m thick) was recovered as part of the ICDP-UNAM-NSF-funded project MexiDrill-Chalco (Brown et al. 2019). In the following sections, we describe the stratigraphy and main lithotypes of the Chalco lacustrine sequence and explore some of the paleoclimate, paleoenvironmental, and basin development implications of this unique sedimentary record.

Basin of Mexico

The Trans-Mexican Volcanic Belt (TMVB) is the largest Neogene volcanic continental arc in North America (160,000 km^2 in extension, 1000 km in length) (Fig. 1) (Ferrari et al. 2012), and is built upon Cretaceous and Cenozoic magmatic provinces (Lugo-Hubp 1984; Lugo-Hubp et al. 1994) The Basin of Mexico is surrounded entirely by volcanic ranges: Sierra de las Cruces to the west includes the oldest geologic formations dated between 3.7 and 0.7 Ma (Delgado-Granados and Martin del Pozo 1993), Sierra de Pachuca and Tezontlalpan to the north (de Cserna et al. 1988), Sierra Nevada to the west (Macías et al. 2012), and Sierra Chichinautzin to the south (Martin del Pozzo 1982; Siebe et al. 2005). Several isolated volcanic structures and clusters are present on the plain, such as Sierra de Guadalupe (García-Palomo et al. 2006) and Sierra de Santa Catarina (Lugo-Hubp et al. 1994; Jaimes-Viera et al. 2018) (Fig. 1).

The Sierra Nevada consists of a chain of andesitic-dacitic stratovolcanoes in a 45 km long N–S alignment, extending from Tláloc in the North (4151 m asl.) to Popocatépetl in the South (5454 m asl.). Iztaccíhuatl (5285 m asl) sits North of Popocatépetl and is composed of a number of coalescing and superimposed edifices that began cone construction ca. 1.8 Ma ago but is now believed to be extinct (Nixon 1989; Macías et al. 2012). Popocatépetl is known to have built upon the remnants of at least three previous edifices (Siebe et al. 1995) with its oldest eruptive products dated since the last magnetic reversal ca. 750,000 years ago. Gravitational collapses, followed by subsequent rebuilding events, have been instrumental in the growth of Popocatépetl to the stratovolcano we see today. The most recent collapse has been dated between 24,000 and 29,000 cal yr BP. During the last 29,000 years, at least eight large Plinian eruptions have occurred in the volcanoes of Sierra Nevada, with seven from Popocatépetl. The Plinian fall deposit of Popocatépetl named "Pómez Tutti Frutti" (Siebe et al. 1997) erupted ca. 17,000 cal yr BP, and is currently the best

stratigraphic marker in the Basin of Mexico (Sosa-Ceballos et al. 2012). It consists of juvenile dacitic pumice and polylithologic lithic componentry making it an easily recognizable fall (Siebe et al. 1995). Since December 21, 1994, activity at Popocatépetl began again, with frequent magmatic eruptions and paroxysms occurring from January 9, 2005. Regularly, tephra and gas are emitted and are visible from the surrounding municipalities. Dome growth and ballistics also pose a significant hazard to those who live around the volcano resulting in an exclusion zones of up to 12 km being enforced by the authorities.

The Sierra Chichinautzin extends from the southern end of the Sierra Nevada to the Nevado de Toluca volcano in the Lerma basin (west of the Basin of Mexico). It is a monogenetic volcanic field with more than 220 volcanic vents consisting of scoria cones and shield volcanoes. Products from these smaller scale volcanoes include lavas and tephra deposits covering an area of ca. 2500 km^2 (Bloomfield 1975; Martin del Pozzo 1982; Lugo Hubp 1984). The compositions of these products are more basic than the nearby polygenetic volcanoes, and generally erupt as andesites with subordinate basalts and dacites defining a calc-alkaline series (e.g. Siebe et al. 2005). The oldest products are 1.2 Ma (Arce et al. 2013a), and the youngest cone is Xitle volcano of an age of 1570 cal yr BP (Siebe 2000).

Among the ranges within the Basin of Mexico, the Sierra de Santa Catarina is prominent and divides the southern Xochimilco and Chalco subbasins from the northern Texcoco subbasin. This range is composed of seven volcanoes aligned E–W, which include cones and a maar with associated lavas and domes of andesitic composition (Lugo-Hubp et al. 1994; Arce et al. 2015). Lugo-Hubp et al. (1994) suggested a Holocene age of Santa Catarina structures based on their relatively young relief; however, $^{40}Ar/^{39}Ar$ dating of its products gives an age between 132,000 and 23,000 years (Jaimes-Viera et al. 2018).

The Nevado de Toluca stratovolcano (80 km to the SW of Mexico City) has had at least one eruption which has dispersed tephra across the Basin of Mexico. This eruption, producing the Upper Toluca Pumice, was Plinian and occurred ca. 12,300 yr BP (Arce et al. 2003). These deposits have been identified and correlated across the Basin of Mexico displaying thicknesses between 12 and 30 cm (Siebe et al. 1999; Ortega-Guerrero et al. 2015).

The Basin of Mexico is a tectonic depression bound by a series of fault systems. The Sierra Chichinautzin is a topographic high of a horst oriented E–W with the Xochimilco and Xicomulco normal fault system as its northern limit and the La Pera normal fault system as its southern limit (Siebe et al. 2004; Alaniz-Álvarez and Nieto-Samaniego 2005; García-Palomo et al. 2008). These extensional faults have served as preferred pathways for frequent, small batches of ascending magma that have successively added altitude to the Sierra Chichinautzin (Siebe et al. 2004). The Sierra de las Cruces was constructed over a N–S alignment and is constituted by three blocks limited by faults oriented E–W and NE–SW (García-Palomo et al. 2008). The existence of NW–SE-oriented normal faults has been inferred from deep wells in Mexico City in the inner part of the basin, crossing most of the metropolitan area. The limestone substrate has been located at different depths at Mixhuca and Tulyehualco wells suggesting the existence of an asymmetric graben limited by

faults dipping to the SE and NW, respectively (Pérez-Cruz 1988). The closure of the ancient southward drainage of the Basin of Mexico by the Sierra Chichinautzin caused the development of a large lacustrine system that spans over the last 1.2 Ma and reached a maximum area of 1690 km^2 at an elevation of 2258 m asl (Ruiz-Angulo and López-Espinoza 2015). Continued subsidence since then has allowed accumulation of a thick sequence (~300 m) of Quaternary lacustrine sediment.

During the Quaternary, Popocatépetl and Iztaccíhuatl supported glaciers; however, a glacial chronology is only available for Iztaccíhuatl (White 1962, 1987), where six advances have been dated by ^{36}Cl between 205,000 and 1000 years ago (Vazquez-Selem and Heine 2011).

Lake Chalco

The lakes in the central Basin of Mexico were drained after the Spanish conquest for flood control, agriculture, and urban development. Documentary evidence shows that during the sixteenth century, prior to these modifications, the lake system covered an area of 1500 km^2 (Ezcurra 1990). Mexico City is built upon these lake beds. Presently, the plain of Lake Chalco is an agricultural region located in the southern subbasin of the Basin of Mexico in which the last remnant of the lake was drained during the late nineteenth and early twentieth centuries. The modern lake at Chalco covers an area less than 40 km^2 (Fig. 1b). It is a small alkaline marsh with an average depth of 3 m with turbid carbonate/bicarbonate, sodium-rich water (Lozano-García et al. 1993; Caballero et al. 2019). Although Lake Chalco falls within the administrative limits of Mexico City, it represents one of the largest remaining blocks of uninhabited land within the megalopolis and thus was identified as a target location for scientific drilling.

Surrounding vegetation has been severely affected by several thousand years of human occupation; the Basin of Mexico is one of the earliest human settlement sites in the Americas, with continuous agricultural activity since the Middle Holocene (Lozano-Garcia et al. 1993; Bhattacharya, and Byrne 2016). The lower elevation parts of the basin are used for agriculture and the foothills are covered by introduced grass and crops. *Pinus* spp. (pine) and *Quercus* spp. (oak) forests are present only in some of the highest areas. Halophytic vegetation currently dominates some of the shallow areas.

Mexico City depends on groundwater for >70% of its water supply. Since the 1950s, much of Mexico City, including the Chalco subbasin, has experienced accelerated ground subsidence with accompanying damage to urban infrastructure as a result of groundwater extraction from the regional aquifer that underlies the thick lacustrine aquitard on which the city is built. By 1991, total subsidence had reached 8 m with subsidence rates exceeding 350 mm/yr (Cabral-Cano et al. 2010). In the Chalco subbasin, these rates exceed 200 mm/yr and have favored the formation of a new lake on top of old lacustrine sediments. The extreme groundwater extraction rates and subsequent high subsidence rates pose a major challenge for a sustainable long-term water supply.

The Valley of Mexico is characterized by a high-altitude subtropical climate, with little temperature variability during the annual cycle and a rainy season from May to October, following the northward Intertropical Convergence Zone ITCZ migration during the boreal summer, although occasional polar fronts can bring precipitation during winter (Mosiño Aleman and Gracia 1974).

Coring the Chalco Basin

(a) *Geophysical surveys*

The subsurface stratigraphy of the Basin of Mexico is known from wells drilled in the metropolitan area to 2–3 km depth (Oviedo de León 1970; de Cserna et al. 1988; Pérez-Cruz 1988; Enciso-De la Vega 1992; Arce et al. 2013b, 2015). The basement rocks are Lower Cretaceous limestones and calcareous conglomerates and anhydrites, most likely of Eocene age. Overlying these deposits are volcanic rocks, which include mostly lavas and less abundant pyroclastic deposits, ages varying from Oligocene to Quaternary. Lacustrine sediments are found interlayered with lavas, breccias, conglomerates, and volcaniclastics. The older lacustrine sediments are present in most wells at depths between 750 and 300 m, although in Copilco-I well a ca. 100 m-thick lacustrine sequence was reported at 1600 m depth (Pérez-Cruz 1988).

A number of geophysical surveys were undertaken prior to the ICDP drilling campaign to characterize the sedimentary infilling of the basin (Brown et al. 2012, 2019). In the Chalco subbasin, near-surface conditions resulting from intensive agricultural development of the area complicate meaningful data collection with conventional seismic reflection surveys. Information from Bouguer gravity anomalies and passive seismic H/V spectral ratio methods, coupled with data from nearby water well logs, indicate the presence of a ca. 300 m "lacustrine sediment" package underlain by ca. 150 to 200 m of "granular material" (Ortiz-Zamora and Ortega-Guerrero 2007). This pattern has been interpreted as a graben bound to the north by the Sierra Santa Catarina and Cerro de la Estrella and to the south by a horst-shaped block composed of the Teuhtli and Xitle volcanoes (Campos-Enriquez et al. 2003). Geophysical surveys (Brown et al. 2012, 2019) provided a map of sediment thickness that was calibrated with measurements of resonance frequencies at the Santa Catarina water wells where the depth to the base of the lacustrine sediment package was known.

(b) *Previous coring campaigns and the ICDP MexiDrill*

In 2008 and 2011, six overlapping cores were drilled to different depths near the depocenter of ancient Lake Chalco: CHA08-II (1–27 m), CHA08-III (1–90 m), CHA08-IV (85–122 m), CHA08-V (29–72 m), CHA08-VI (70.8–85 and 106–122.4 m), and CHA11-VII (18 m). The cores CHA08 III to VI were drilled with a Shelby corer in 1.10 m sections with inner 10 cm diameter PVC tubes. The cores CHA08-II and CHA11-VII were drilled with a modified Livingstone piston corer in 1 and 2 m long sections.

The ICDP MexiDrill project goal was to recover the complete lake sequence of the Chalco Basin. During 6 weeks of continuous work in March–April 2016, the MexiDrill field campaign recovered more than 1000 m of drill core using wireline diamond coring techniques in four holes at a site identified by a suite of techniques as described above as the location of the thickest lacustrine sequence (Lozano-Garcia et al. 2017). The drillers, through rotational drilling techniques, reached depths of 420 m in core 1A, 310 m in 1B, and 520 m in 1C. Core 1D used a piston corer with percussion to enhance recovery of the upper soft sediments. A total of 1152 m of core sediments was recovered reaching a maximum depth of 520 m. Recovery ranged from 88% to 92% in the three cores (Fig. 2).

The upper 300 m of core 1A is composed of fine-grained lacustrine sediments alternating with discrete tephra layers, and the lower sections (ca. 300–422 m) are composed of volcaniclastics and lavas. Full downhole geophysical logs were collected from hole 1A. Cores 1B and 1C recovered the upper lacustrine sequence (313 m), and 1C continued through the volcaniclastic-lava unit reaching poorly sorted, coarse clastic deposits (ca. 512–520 m). Triple core recovery with offset core intervals in the upper 300 m lacustrine unit provides sufficient core overlap to create a composite sequence and continuous paleoenvironmental and volcanological reconstructions. In total, the project drilled 1262 m (including reamed sections) and recovered 1065 m of cores. (Fig. 2). The composite sequence is 554 mc (composite depth in meters) long including 52 m (9.4%) of gaps, mainly occurring within the lower coarse-grained volcaniclastic deposits, which were difficult to recover.

Lacustrine Facies

A number of clastic, carbonate, biogenic, chemical, and volcanic facies were defined in the Chalco 2008 cores (Herrera-Hernandez 2011). Clastic facies were composed of clay or silt with variable amounts of organic matter, varied colors (black brown, reddish), and with laminated, banded, and massive textures. Discrete occurrences of struvite (hydrated magnesium-ammonium phosphate) were identified at several levels. Biogenic facies included thin layers of diatomaceous ooze, thick layers of diatomaceous, organic-rich mud, and about 15 layers, between 5–10 cm thick, of ostracod-rich intervals. These composed more than 80% ostracod carapaces (ostracod *hash*). In the lower part of the sequence (between 113 and 122 m), up to 11 layers about 3–5 cm thick of carbonate mud mostly composed of endogenic carbonates (Mg-calcite, dolomite, and siderite) occurred. A number of tephra layers (lapilli and ash) were described and identified.

In the 2016 ICDP cores, lithotypes were defined based on lithologies and textures determined by macroscopic and microscope (smear slide) observations (Schnurrenberger et al. 2003; Table 1 and Fig. 3). In Table 1, the main features of the lithotypes are summarized and their associated depositional processes and environments interpreted. Figure 3 shows core images of selected intervals illustrating the main lithotypes identified in the MexiDrill cores.

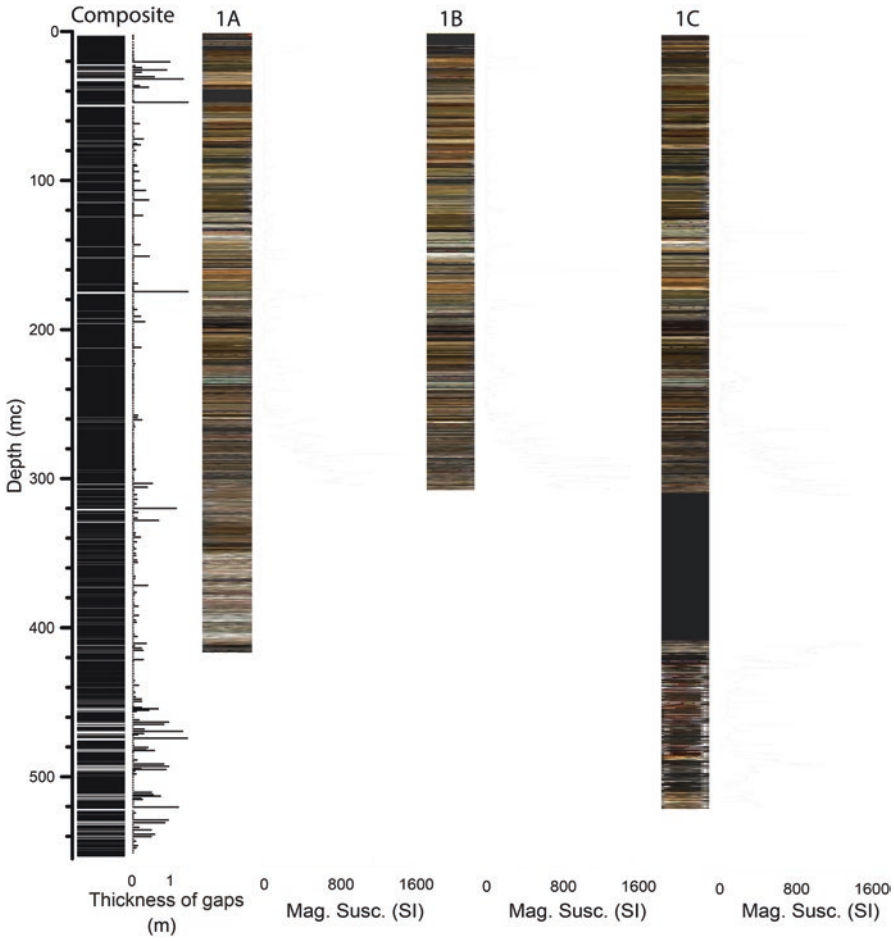

Fig. 2 Composite record from the Chalco drill cores and the ICDP MexiDrill cores including magnetic susceptibility and stacked color core images of the sections for site 1 cores (holes A, B, and C). White colored gaps of the composite record in the vertical column are given in thickness (m) by the bar chart

Total organic carbon (TOC) and inorganic carbon (TIC) analyses of selected samples are consistent with the three main types of lacustrine lithotypes: carbonate, organic, and diatomaceous (Fig. 4). The five main groups of lithotypes are:

- Organic. This includes: (i) organic-rich silty clay, (ii) sapropelic silty clay, and (iii) peat. The TOC range is quite large (up to 45%) and the TIC is below 1% in most samples.
- Diatomaceous. These are diatomaceous silty clays and include (i) laminated, (ii) banded, and (iii) "mottled" lithotypes. TIC content is generally lower than 1% and TOC reaches up to 4%.

Table 1 Chalco Basin lithotypes defined in the MexiDrill sequence: description, total thickness (in meter and percentage), and depositional processes and environments

Lithotypes	Description	Thickness	Depositional processes and environments
Organic-rich (O)	Organic-rich silty clay, banded or mottled in layers up to several dm. Organic matter includes sponge spicules, phytoliths, diatoms as well as terrestrial and amorphous aquatic OM. Lithotypes range from peaty to organic-rich silty clays. Some intervals contain abundant terrestrial OM clasts and variable amount of volcanic glass.	18 m 3.3%	Swamp/wetland to relatively shallow (and small) eutrophic lacustrine environment
Diatomaceous laminated (Dl)	Finely laminated diatomaceous silty clay with couples of light beige and dark brown laminae, light laminae (1–2 mm) contain almost only diatoms, dark laminae (2–5 mm) contain more clastic components. Thickness ranges from few cm to several dm.	44 m 7.8%	Relative deep and distal fresh-water lake undergoing strong likely seasonal changes and a at least partly anoxic water column Light laminae reflect deposition during diatom blooms Dark laminae reflect baseline deposition in the distal areas of the lake
Diatomaceous banded (Db)	Thin to medium bedded diatomaceous silty clay intercalated often by gray siliciclastic-rich 2–5 mm thin clay beds	80 m 14.4%	Distal, deep lake environments dominated by fine clastic and diatom deposition. Gray layers deposited during flood events transporting material from littoral areas and/or watershed.
Diatomaceous mottled (Dm)	Diatom-rich clayey silt with speckle of beige diatom clasts in a relatively homogenous matrix	1 m 0.2%	Distal but shallower environments with redox fluctuations responsible for mottling textures.
Carbonated banded (Cb)	Dm-thick beds composed of autochthonous carbonate minerals (Aragonite, Calcite), ostracod shells, few diatoms with etched surfaces and minor organics remains and clastic minerals; reddish intervals contain coarser carbonate grains, light gray intervals are Ostracod and Phacotus rich; dark gray intervals have more fine-grained (micritic) carbonate grains	57 m 10.4%	Shallower alkaline/ brackish environment dominated by carbonate precipitation and high biogenic productivity with fine carbonate clastic input from littoral areas

(continued)

Table 1 (continued)

Lithotypes	Description	Thickness	Depositional processes and environments
Carbonated massive (Co)	Mm to cm thick laminae composed mostly of biogenic or autochthonous carbonate material. Some dominated by ostracod shells and Phacotus (few layers almost purely of ostracod shells). Some are cemented if directly overlaying a v-layer	8 m 1.4%	Rapid carbonate deposition by endogenic processes (carbonate minerals) or biogenic accumulation (ostracods) in a highly productive system with limited detrital input
Coquina (C)	Bivalves, gastropods, and ostracods within a diatomaceous-silty clay matrix	0.6 m 0.1%	Biogenic accumulation in littoral areas
Silty clay (Sc)	Medium to thick beds of light gray silty clay dominated by silicate minerals and with variable diatom and carbonate minerals	18 m 3.2%	Distal, deep lake environments dominated by fine clastic deposition and with low bioproductivity
Sand (S)	Fine to coarse sand (carbonate, volcanic clasts) with silty clay matrix	1.4 m 0.2%	Alluvial (or close to alluvial-influenced lacustrine littoral) high-energy environment during a relatively low lake stand
Gravel (G)	Clast-supported, coarse sand matrix with rounded heterolithic pebbles, in massive, graded, and laminated layers		Alluvial /Fluvial, high-energy environment during relatively low lake stands
Tephra (T) and Lapilli (L)	Fine ash to lapilli pumice beds with sharp boundaries to over- and underlying silty clays		Reworked or fallout volcanic deposits from a volcanic source in vicinity to the lake
Volcaniclastic (V)	Coarse deposits (from gravel to sand) composed only of volcanic rock fragments and volcanic material matrix. Mostly matrix-supported; some clast-supported; massive, banded, and laminated structures. Dm to meter thick layers.	207.1 m 37.4%	Primary coarse volcaniclastic deposits and reworked volcanic materials by slope-failure, alluvial, mass wasting, and fluvial processes
Basalt (B)	Black to reddish vesicular Basalts	68.4 m 12.4%	Lava flows

- Calcareous. These are carbonate-bearing silty clay and include (i) banded and (ii) massive lithotypes. A unique lithotype is an ostracod and mollusk-rich hash or coquina at the base of the lacustrine sequence. Carbonate content covers a wide range, from 1% to almost 100% in some thin layers.
- Clastic. These include silty clay.
- Volcanic. These occur as (i) volcaniclastic layers as relatively thin tephra layers (ash and lapilli) and clastic deposits and (ii) lavas).

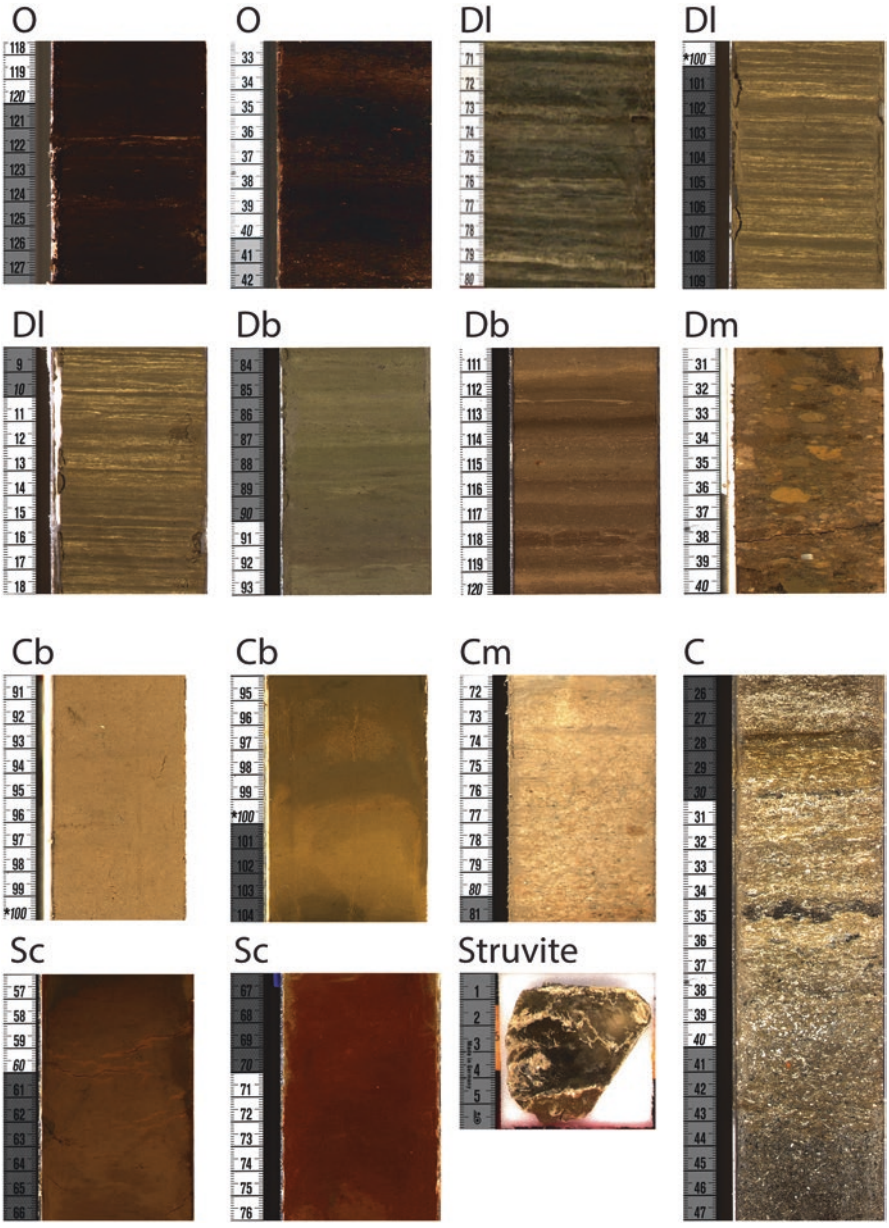

Fig. 3 (**a**) Core images of main lithotypes; vertical scale in centimeters: Organic-rich (O, MEXI-CHA16-1C-133Y-1 117.5–127.5 cm, MEXI-CHA16-1A-76Y-1 32–42 cm); Diatomaceous laminated (Dl; CHA08-VI-18 70–80 cm, MEXI-CHA16-1C-140Y-1 99–109 cm, MEXI-CHA16-1B-147Y-1 8–18 cm); Diatomaceous banded (Db, MEXI-CHA16-1A-169Y-1 83–93 cm, MEXI-CHA16-1C-167Y-1 110–120 cm); Diatomaceous mottled (Dm, MEXI-CHA16-1D-10C-2 30–40 cm); Carbonated banded (Cb, MEXI-CHA16-1D-11C-13 90–100 cm, MEXI-CHA16-1C-32Y-1 94–104 cm); Carbonated massive (Co, MEXI-CHA16-1C-174Y-1

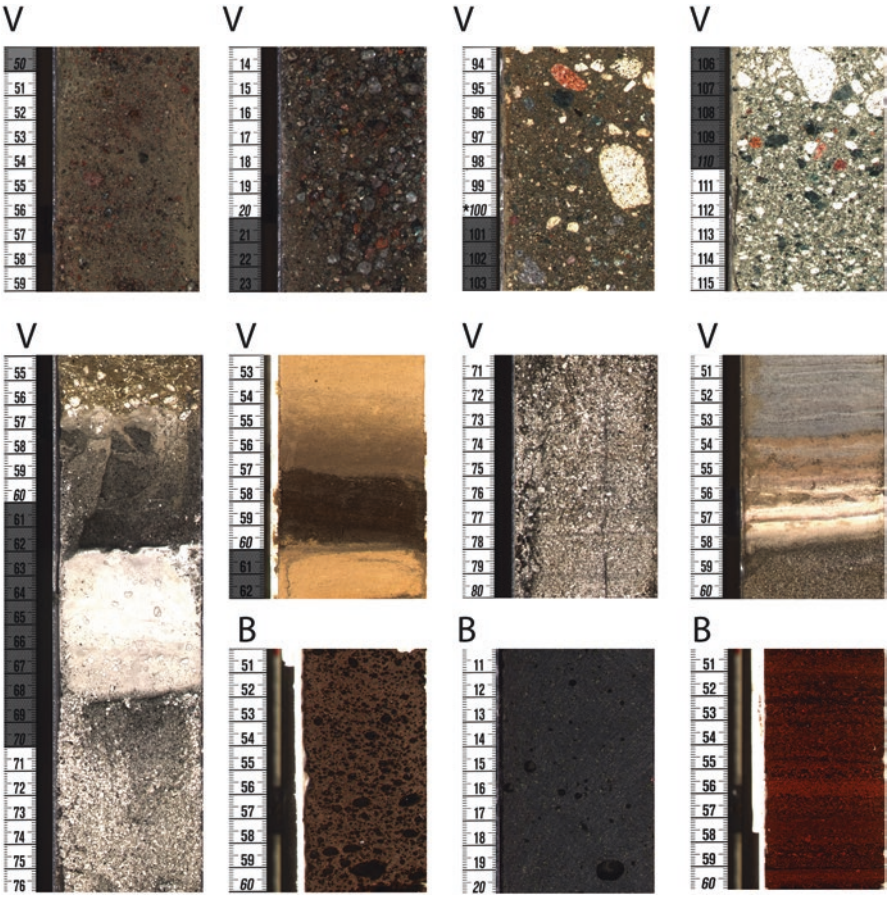

Fig. 3 (continued) 132–142 cm); Coquina (C, MEXI-CHA16-1A-175Y-1 25–47 cm); Silty clay (Sc, MEXI-CHA16-1A-27Y-1 56–66 cm, MEXI-CHA16-1A-54Y-1 66–76 cm); Struvite (MEXI-CHA16-1C-18Y-1). (**b**): Core images of main lithotypes; vertical scale in centimeters Volcaniclastic (V, MEXI-CHA16-1C-178Y-1 49–59 cm, MEXI-CHA16-1C-182Y-1 13–23 cm), MEXI-CHA16-1A-269Y-1 93–103 cm, MEXI-CHA16-1A-271Y-1 105–115 cm, MEXI-CHA16-1A-175Y-1 54–76 cm, MEXI-CHA16-1D-8C-2-A 52–62 cm, MEXI-CHA16-1B-181Y-170–80cmandMEXI-CHA16-1B-177Y-150–60cm);Basalt(B,MEXI-CHA16-1C-231Y-1 50–60 cm, MEXI-CHA16-1C-217Y-3 10–20 cm, MEXI-CHA16-1C-270Y-1-A 50–60 cm)

Along the sequence, these main lithotypes show associations at several scales. At a decimeter scale, alternation of sapropelic, diatomaceous, organic (peat), and carbonate facies are common. Lithotypes group in thicker (multimeter scale) intervals that define lithostratigraphic units (see next section) and illustrate dynamic changes of the lacustrine basin encompassing a mosaic of depositional environments: shallow alkaline carbonate-producing lakes, deeper lakes with diatomaceous

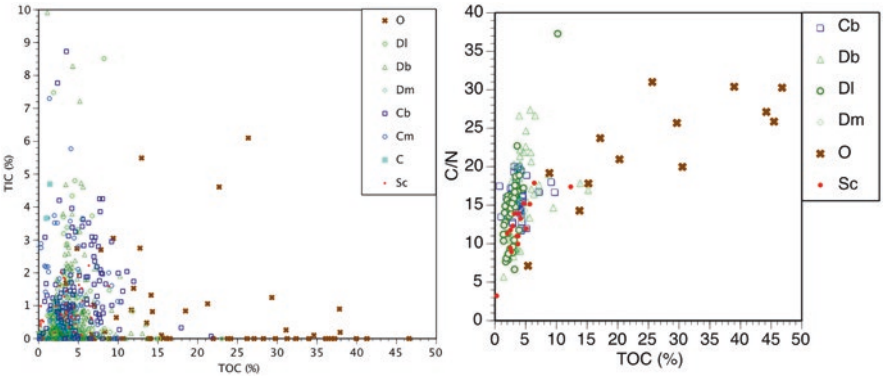

Fig. 4 (**a**) Total Inorganic Carbon (TIC) contents plotted against Total Organic Carbon (TOC) contents of main lithotypes: carbonate (blue boxes), organic (brown open circles), and diatomaceous (pink crosses) clayey silt. (**b**) TOC plotted versus C/N for the main lithotypes: carbonate (blue boxes), organic (brown open circles), and diatomaceous (pink crosses) clayey silt

deposition, wetlands with peat accumulation, and lakes dominated by organic deposition (sapropelic muds).

Stratigraphy of the Chalco Basin

Previous Stratigraphies Based on five shorter sediment cores, an initial stratigraphy was defined by Ortega-Guerrero (1992) for the upper 26 m of the sequence. The top unit 1 (0–1.8 m) is composed of brown silt with altered lapilli fragments, and more abundant ostracod and plant remains toward the base. Unit 2 (1.8–2.5 m) includes brown silt with abundant plant remains and ostracods. Unit 3 (2.5–3 m) includes diatomaceous facies with intercalated tephra intervals. Unit 4 (3–8 m) is composed of dark brown to black peat with abundant tephra layers. Brown silt dominates the lower units (5 to 7): with more plant fragments in Unit 5 (8–11 m), more gastropod shells in Unit 6 (11–16 m), and more ostracod levels and abundant lapilli layers in Unit 7 (16–26 m). The "Gran Ceniza Basáltica" at 21 m depth provides an important chronostratigraphic marker for the sequence (older than 31 ka, Ortega – Guerrero et al. 2015, 2017, 2018). Other key tephra layers are identified, including: Pómez Ocre (ca. 5 ^{14}C kyr); "Pómez Toluca Superior" or "sal y pimienta" (12,520 +/− 135 ^{14}C yr, Arce et al. 2003); "Pómez con Andesita" (ca. 14 ka) and "Pómez Tutti Frutti" (17,600 cal ka BP), Sosa Cebalos et al. 2012).

After the 2008 drill campaign, a new stratigraphy was developed for the upper 125 m with five main units (Herrera 2011): Unit 1 (0–8 m) groups organic-rich clay and silt and diatomaceous facies with several tephra layers. Unit 2 (8–68 m) is dominated by yellowish brown clayey silt (massive, banded, laminated) with more mottled intervals (subunit 2A (8–40 m)) and more frequent intercalation of gray silty clay layers (subunit 2B, 40–68 m). Unit 3 (68–90 m) contains olive brown and olive

clay-silt with some thick intervals of reddish-brown silts and the presence of struvite (Fig. 3a) at some levels. Unit 4 (90–104 m) is characterized by the occurrence of olive brown clay-silt with some diatom ooze layers. Unit 5 (104–124 m) is defined by the abundance of laminated facies with alternation of carbonate-rich layers, diatomaceous facies, brown, gray clayey silt, and olive brown clayey silt.

A. *ICDP MexiDrill lithostratigraphy*

The 2016 ICDP MexiDrill drilling campaign obtained four long drill cores in the Chalco Basin, reaching up to 553 mc (composite depth) in the volcanic basement, and recovering the entire lake sequence (upper 295 mc). Magnetic susceptibility values supported correlation of the drill cores (Fig. 2). Cores were split and imaged at LacCore/CSDCO (University of Minnesota) and further correlation was achieved by visual stratigraphy using the CoreWall software. A 554 mc long spliced sequence was generated including core section from both the 2008 and 2016 projects. Eighteen lithological units have been defined (Table 2) based on lithotypes and magnetic susceptibility values (Fig. 5). The upper five units correspond to those defined in 2008 cores. The depth boundaries are those from the spliced composite core. Furthermore, a composite corrected depth scale (mcc) was developed to reflect relatively constant background lacustrine sedimentation by collapsing volcanic layer depths to zero thickness to account for instantaneous event deposition. Similar approaches have been used within other lake drilling records facing frequent volcaniclastic input (Deino et al. 2019; Stockhecke et al. 2014). The composite-corrected sequence totals in 241.68 mcc (Fig. 6).

Unit 1 (0–15 m) groups organic and diatom-rich lithotypes with relatively low clastic mineral content and includes a number of volcanic tephra that are well-correlated in the basin. It corresponds to Units 1 to 4 as defined by Ortega-Guerrero (1992) and Unit 1 as defined in the 2008 cores. A conspicuous black diatomaceous interval includes the Pómez Toluca Superior (also known as "Sal y Pimienta") tephra. The laminated and silty clay and dark brown massive and banded silty clay include some peat layers, and the Tutti Frutti Tephra is present in this unit as well. The environments associated with these lithotypes are relatively shallow lacustrine settings dominated by organic and diatomaceous sedimentation.

Unit 2 (15–90 m) is characterized by carbonate lithotypes. It broadly correlates with Unit 2 in the 2008 cores. The upper unit 2A (15–53.5 m) corresponds to Units 5 through 7 (Ortega-Guerrero 1992) and is dominated by banded calcareous lithotypes. Subunit 2B (53.5–90 m) contains more grayish- and greenish-brown calcareous clayey silt and the terrigenous content is higher with common fining upward sequences. Subunit 2A groups light brown/yellowish banded diatomaceous and calcareous silty clay with plant fragments, gastropod shells, and some ostracod-rich levels and mottled intervals. It also includes the "Gran Ceniza Basáltica" tephra. Facies in Unit 2 have textures indicative of shallow lake levels with occurrence of soft clasts, subaerial cracks, and mottling. Periods of higher terrigenous content suggest higher run-off or discrete flooding episodes; more alkaline conditions were conducive to periods with more abundant ostracods. Frequent cm-thick Fe-stained intervals suggest shifting in redox conditions during early diagenesis.

Table 2 Main lithostratigraphic units (as shown in Fig. 5) defined in the composite MexiDrill sequence using corrected composite depth (mc). The thicknesses of the main units in core 1A are also indicated

Unit	Dominant lithotypes	Base of unit (mc) Splice composite	Thickness (core1A)
1	Organic and diatomaceous (laminated, massive)	15	13.02
2A	Diatomaceous and calcareous (banded)	53.5	32.36
2B	Calcareous and diatomaceous (banded), more gray silt toward the base	90	30.39
3	Diatomaceous (laminated), calcareous and diatomaceous (banded)	103	11.92
4	Diatomaceous (laminated)	150	43.42
5	Volcaniclastic (mottled)	164	10.68
6	Calcareous, volcaniclastic, diatomaceous, and organic	174	9.51
7	Diatomaceous (laminated)	190	11.99
8	Calcareous	204.5	13.56
9	Diatomaceous (laminated)	210.8	5.6
10	Volcaniclastic (with some intercalated lake sediments)	218	18.53
11	Organic, calcareous, and diatomaceous	236.6	9.73
12	Diatomaceous (laminated) and organic	256.5	18.36
13	Volcaniclastic	269	14.87
14A	Volcaniclastic and diatomaceous		5.76
14B	Calcareous/Diatomaceous (laminated)		6.59
14C	Diatomaceous (laminated) and organics	292	10.54
15	Volcaniclastic, clastic, and diatomaceous	317	22.6
16	Volcaniclastic	447	128.48
17	Basalt lava	541	92.04
18	Volcaniclastic	555	12.15

Fig. 5 The complete synthetic lithostratigraphy of the spliced sequence of MexiDrill including 2008 and 2016 cores on composite depth (mc) on the right and the magnification into the acustrine sequence covering the upper 295 mc on the left. Preliminary age constraints all transferred on the composite depth consist of correlated previously ^{14}C-dated tephras (in gray text; the "Great Basaltic Ash" (older than 34 ka) (Ortega Guerrero et al. 2015, 2017, 2018), the "Pómez Toluca Superior (PTS)" dated as 12,520 +/− 135 14C yr BP (Arce et al. 2003), the "Pómez Tutti Frutti (PTF)" as 17,670 cal ka BP (Sosa-Ceballos et al. 2012) and "White pumice (WP)" as 27,800 cal BP (Siebe et al. 2017)). Radiocarbon dates of pollen (in green text, Ortega-Guerrero et al. 2018; Lozano-García et al. 2015), a U/Th date of zircon grain selected from tephra (in red text, Ortega Guerrero et al. 2017; Torres-Rodriguez et al. 2018), and a new U/Th age from lacustrine micritic carbonate (in blue text)

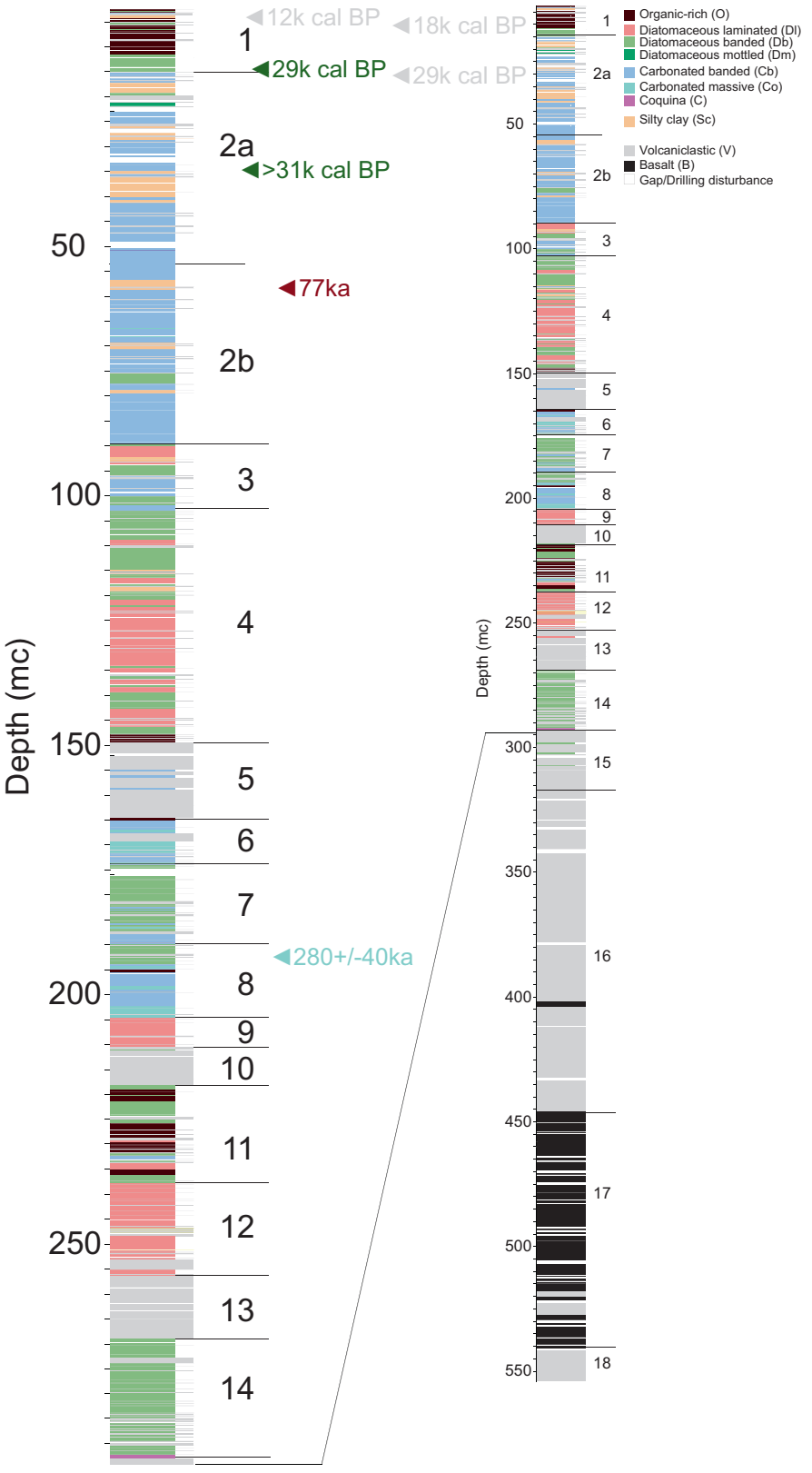
Depth (mc)
50
100
150
200
250
1
2a
2b
3
4
5
6
7
8
9
10
11
12
13
14
12k cal BP
18k cal BP
29k cal BP
29k cal BP
>31k cal BP
77ka
280+/-40ka
Depth (mc)
50
100
150
200
250
300
350
400
450
500
550
1
2a
2b
3
4
5
6
7
8
9
10
11
12
13
14
15
16
17
18
Organic-rich (O)
Diatomaceous laminated (Dl)
Diatomaceous banded (Db)
Diatomaceous mottled (Dm)
Carbonated banded (Cb)
Carbonated massive (Co)
Coquina (C)
Silty clay (Sc)
Volcaniclastic (V)
Basalt (B)
Gap/Drilling disturbance

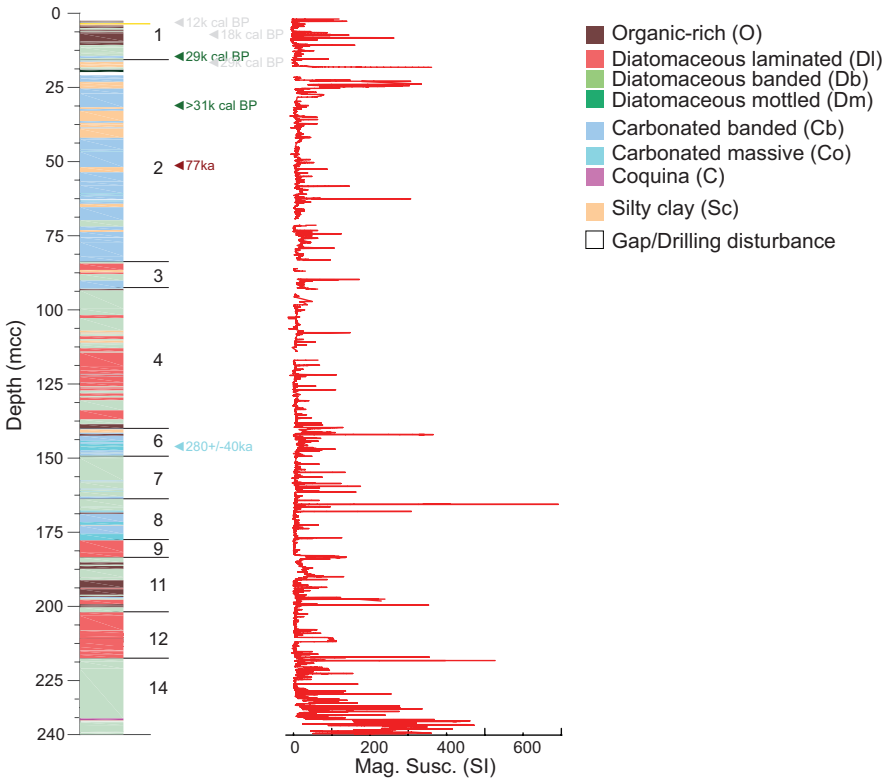

Fig. 6 The lithostratigraphy of the MexiDrill record on the composite corrected depth (mcc). Volcaniclastic layers have been collapsed in this version to show only the lacustrine sediments. Legend is shown in Fig. 5

Unit 3 (90–103 m) is characterized by the occurrence of carbonate and diatomaceous laminated lithothypes, with some reddish-brown carbonate silts. This unit presents several organic-rich levels with struvite occurrences that have been interpreted as guano accumulation during hyper-productivity phases (Pi et al. 2010). Reddish intervals have higher MS values and represent oxidized facies, likely during early diagenesis. The large facies variability (saline and freshwater diatoms, mottling, periods of high clastic input) points to significant hydrological changes during relatively low lake levels.

Unit 4 (103–150 m) is defined by the occurrence of alternations of finely laminated diatomaceous, carbonate, banded diatomaceous, and organic-rich lithotypes. Finely laminated facies are indicative of deeper lake environments and more frequent suboxic conditions. Carbonate deposition reflects periods with higher alka-

linity, but still during relatively high lake levels as suggested by the finely laminated facies.

Unit 5 (150–164 m) is a volcaniclastic unit, composed of massive volcanic material with abundant secondary textures such as nodules, cracks, and staining. This may suggest subaerial deposition and/or reworking by surface processes of pyroclastic deposits, e.g., ignimbrites or lahars. The unit is topped by a tephra layer.

Unit 6 (164–174 m) is characterized by the occurrence of calcareous lithotypes (variegated, banded to laminated). They alternate with massive brown silty clays at the top and with laminated diatomaceous and more organic-rich intervals with secondary Fe-staining toward the base. A thick volcanic interval occurs in the middle of the unit.

Unit 7 (174–190 m) groups laminated to banded greenish diatomaceous silty clay and *Unit 8 (190–204.5 m)* contains carbonate-rich, massive, and banded lithotypes, with some reddish and brownish intervals.

Unit 9 (204.5–211 m) is composed of greenish laminated diatomaceous silty clay with more dark brown intervals toward the base.

Units 6 to 9 are arranged in alternating carbonate and diatomaceous units, as Units 6 and 8 are dominated by calcareous lithotypes, while Units 7 and 9 mostly include diatomaceous ones.

Unit 10 (211–220 m) is a thick volcaniclastic unit that includes two lake sediment intervals (organic-rich and diatomaceous silty clay).

Unit 11 (224–236.5 m) and *Unit 12 (236.5–256.5 m)* are composed of alternating organic-rich lithotypes (peaty silty clay) and diatomaceous (dark brown, massive diatomaceous silty clay) with some reddish banded carbonate and silty clay. In Unit 12, diatomaceous silty clay is dominant (with some greenish/brownish, banded/laminated intervals). Banded, brownish intervals are more frequent toward the base, then grading into greenish and better laminated.

Unit 13 (256.5–269 m) is a volcaniclastic unit with intercalated diatomaceous layers and tephra at the bottom.

Unit 14 (269–292 m) includes diatomaceous lithotypes with tephra layers, more abundant at the top, brownish/reddish, banded carbonated and laminated diatomaceous lithotypes, and dark brown diatomaceous silty clay intervals in the middle and laminated diatomaceous silty clays and oozes at the bottom At the base, a unique decimeter-thick ostracod and mollusk-rich layer (coquina) is found on top of a white pumice tephra, with overlying ash.

Unit 15 (292–317 m) contains interbedded m-thick fine volcaniclastic intervals, coarse clastic lithotypes deposited by mass transport, alluvial and fluvial processes, and dm-thick laminated brownish diatomaceous silty clay. The top volcaniclastic layer is a conspicuous white, laminated, pumice-rich layer.

Units 16 to 18 are the basal volcanic and volcaniclastic units.

Unit 16 (317–447 m) is a thick volcaniclastic unit composed of m-thick subunits, displaying polylithologic clasts among a matrix of varying coarseness.

Unit 17 (447–541.7 m) is composed of lava with laminated, massive, vesicular textures.

Unit 18 (541.7–551 m) is a volcaniclastic unit, with distinct clastic horizons. Largely, the deposit appears to be fining with stratigraphic height.

Evolution of the Chalco Basin

(a) *Depositional evolution*

The lower 200 m of the Chalco sequence are composed of volcaniclastic deposits and lavas. The volcaniclastic deposits of basal unit 18 could be associated with a period of volcanic activity at the end of the volcanic-tectonic phase responsible for the formation of the modern Chalco Basin. Emplacement of nearly 100 m of lava with vesicular textures (unit 17) followed this early episode of volcanic activity. Additional volcanic events occurred leading to the deposition of a thick interval (almost 130 m) of volcaniclastic facies (unit 16) that continued with the infilling of the Chalco Basin. Thick, massive layers of coarse to fine matrix-supported clasts were deposited as alluvial activity dismantled either existing volcanic structures or deposits associated with major evolution events from nearby polygenetic volcanoes.

Unit 15 represents the onset of the infilling of the newly formed Chalco Basin by lacustrine depositional processes. This interval has been described and interpreted in detail by Martinez-Abarca (2019) and Martínez-Abarca et al. (2021). During this period, input of volcaniclastic material continued. Later on, increased efficiency of erosion is indicated by the occurrence of rounder clasts and clast-supported textures in clast-rich sections. Smaller sizes and fine lamination textures in the finer-grained layers indicate an increased influence from a hydrologic regime. A fluvial-lacustrine setting is interpreted as the depositional environment for the upper part of unit 15, followed by the final development of the Chalco Lake (Martínez-Abarca et al. 2021). The lacustrine phase in the Chalco Basin started at the top of unit 15 with deposition of banded diatomaceous silty clay intercalated with fluvial deposits. Diatom assemblages indicate freshwater conditions in this newly formed lake (Martínez-Abarca et al. 2021). The intercalation of lacustrine and alluvial facies suggests that the alluvial and fluvial drainage networks carved the volcanic watersheds and connected to the lake environment. A relatively large number of tephras interbedded with the lake sediments suggest a high frequency of explosive eruptions occurred which transported deposits to the Chalco region. The occurrence of a unique ostracod, mollusk, and gastropod coquina (Unit 14C) indicates periods of high bioproductivity in freshwater with the presence of hard substrates on the lake floor. A stepwise development with early shallow lake stages have been described in other volcanic basins (Pueyo et al. 2011; Martínez-Abarca

et al. 2021). Higher lake levels and deeper environments led to deposition of laminated diatomaceous lithotypes (unit 14 B and A). Unit 13 demonstrates volcanic activity was key producer of material here, leading to the deposition of more volcaniclastic deposits. Lake deposition continued with laminated diatomaceous and organic facies (Units 12 and 11) interrupted by deposition of another thin volcaniclastic interval (Unit 10). Fine-grained lake deposition continued with alternating diatomaceous (Units 9 and 7) and carbonate (Units 8 and 6) dominated phases. After emplacement of another volcaniclastic interval (Unit 5), the lake deepened and laminated carbonate, diatomaceous, and organic lithotypes (Unit 4) were deposited indicative of more anoxic, alkaline, and productive conditions. Deposition of banded to massive facies dominated Unit 3, suggesting relatively low lake levels. The top of this unit marks the last deposition of finely laminated diatomaceous facies.

Unit 2 is dominated by carbonate lithotypes and some silty facies which demonstrate high magnetic susceptibility. During deposition of Unit 2, lake levels continued to be relatively shallow and the lake experienced periods of higher alkalinity, conducive to precipitation of carbonates and deposition of some layers with abundant ostracods and gastropods. Terrigenous content progressively increased toward the top as indicated by higher magnetic susceptibility values and higher clastic content. The presence of intense mottling and root structures suggests multiple episodes of extremely low lake levels with subaerial exposure of the sediment at this site.

Unit 1 represents deposition in a lake dominated by sedimentation of organic-rich clay, silt, and diatomaceous facies. During this period, biogenic activity dominated over detrital watershed input.

(b) *Paleoenvironmental, paleovolcanism, and paleoclimate implications*

A preliminary chronological framework for the Chalco sequence has been established using a variety of dating techniques in several cores (Herrera 2011; Torres-Rodriguez et al. 2015, 2018; Martínez-Abarca 2019; Caballero et al. 2019) including:

- tephra layers: the Pómez Ocre (ca. 5 ^{14}C kyr), the Upper Toluca Pumice (UTP, 12,520 +/− 135 ^{14}C yr) (Arce et al. 2003), the Tutti Fruti Pumice (TFP, 17,670 cal ka BP) (Sosa-Ceballos et al. 2012), the "Great Basaltic Ash" (older than 34 ka), the "Pómez con Andesita" (ca. 14 ka) (Ortega Guerrero et al. 2015, 2017, 2018), and the White pumice (WP, 27,800 cal BP) (Siebe et al. 2017).
- Radiocarbon ages in pollen extracts from samples of the upper units (Ortega Guerrero et al. 2017; Torres-Rodriguez et al. 2018).
- U/Th date (76.74 ka) obtained from zircons collected from an ash layer at 69.84 mcc (75.28 mc in the MexiDrill-Chalco composite sequence) (Ortega Guerrero et al. 2017; Torres-Rodriguez et al. 2018).
- U/Th date obtained from a micritic carbonate sample containing few ostracods from 192.63 mc (165.73 mcc) (CHA16-1C_107Y-1 5.5 to 7.5 cm) yielding an age of 280 +/− 40 ka.

Extrapolation of sedimentation rates based on these preliminary chronological constraints suggests that onset of lacustrine deposition (top of Unit 15, 240.34 mcc, 309.15 mc) occurred between 364 and 505 ka, suggesting that the MexiDrill record will extend back to MIS 10 or MIS 13. This basal date was estimated by linear extrapolation of the two U/Th dates (zircon at 69.85 mcc and carbonate at 165.73 mcc) and considering the 40 ka error for the carbonate U/Th age. Ongoing work using 40Ar/39Ar dating of tephra and more radiocarbon dates in upper cores will refine this chronology. More saline diatom assemblages in diatomaceous facies and the occurrence of carbonate lithotypes and organic-rich layers suggest more arid conditions during interglacials, whereas higher humidity during glacial stages is indicated by freshwater diatom assemblages and the occurrence of finely laminated diatomaceous facies.

This preliminary view of glacial–interglacial conditions is consistent with the mid-Pleistocene sequence from Valles Caldera, New Mexico (Fawcett et al. 2011). In that sequence, the driest conditions occurred during the warmest phases of interglacials, with a significant reduction in summer precipitation, possibly in response to a poleward migration of the subtropical dry zone. In the South American tropics, the Lake Titicaca sequence showed a distinctive pattern during the last 400 ka of clastic, glacial-related facies deposited during wetter periods associated with glacier advances and relatively high lake level stages, and more carbonate-rich facies deposited in shallower conditions during warmer and relatively less humid interglacials (Fritz et al. 2007). In the shallow Lake Junín system, depositional variability during the last 700 ka is characterized by alternating intervals of carbonate lake-wetland facies (interglacial periods) and clastic-facies (glacial) (Cheng et al. 2020).

For the last glacial cycle, the age model is more robust. A number of studies in Lake Chalco indicate that the lake had high salinity prior to 27 ka BP and during the Last Glacial Maximum (LGM, 23 to 17 ka cal BP), and then deepened during the deglaciation, between 15 and 11 ka BP. During the Early Holocene, the lake became shallower and saline. These results suggest that lake chemistry is highly controlled by evaporation, with low evaporation periods, such as the LGM, showing lower salinity than intervals with high evaporation (end of MIS 3 and early MIS 1) which are saline. However, at Chalco, the LGM (27–15 ka cal BP) shows lower lake level conditions compared to the late glacial, consistent with lower fluxes of terrigenous material into the Cariaco Basin (Peterson et al. 2000).

In contrast, the results from the scientific drilling in Lake Peten Itza (ICDP PISDP project, Yucatan Peninsula, Guatemala) (Hodell et al. 2006) showed wet conditions during the Last Glacial Maximum, a transition to drier conditions during the late Glacial (including the Younger Dryas), and a generally wet Holocene, illustrating an opposite trend at the orbital scale. Interestingly, during the last 40,000 years at a millennial scale, the Chalco record has been interpreted to show a pattern of cold and dry conditions during colder northern hemisphere periods (stadials), comparable to other tropical northern hemisphere sites, further supporting the idea that

there is a strong coupling between tropical and North Atlantic regions (Caballero et al. 2019).

Volcanic activity has played a significant role in the origin and evolution of Lake Chalco. Multiple eruptions from a variety of source volcanoes are present within the record. Early volcanic output (Units 18 to 15, Fig. 5) was responsible for the deposition of over 200 m of volcanic and volcaniclastic material that originated and partially filled the basin. From Unit 13, over 16 m of primary and reworked tephra was deposited during a mostly stable lacustrine setting. From Unit 10, over 19 m of volcanic deposits occur within the core and from Unit 5, there is ca. 11 m of volcanically derived deposits. From Unit 2, volcaniclastic input had ceased, but many discrete tephra layers 1–50 cm can be identified; two of which are from well-documented eruptions from Popocatépetl and Nevado de Toluca volcanoes. Uplift of the Santa Catarina Sierra and the Chichinautzin Sierra volcanoes have mostly likely contributed to higher sediment input from these watersheds. Ortega-Guerrero et al. (2015) suggest that the monogenetic volcano Teuhtli, in the southwestern part of the Chalco lacustrine plain, is the origin of the so-called Gran Ceniza Basáltica tephra (dated older than 34 ka, Ortega Guerrero et al. 2015, 2017, 2018). Volcanic input occurred during the last 23 ka from Santa Catarina to the north, Xico to the east, and Teuhtli volcano to the west and are mostly likely sources of some of these tephras. Ongoing work on the tephrastratigraphy and volcanological history of the Mexico City region aims to address the volcanic contributors to the Basin of Mexico and their associated hazard implications for the region today.

Conclusions

The cores from the Basin of Mexico provide a continuous lacustrine record from tropical North America for the Upper Pleistocene and the early to mid-Holocene, including several glacial cycles and volcanic events. The >500 m long MexiDrill sequence illustrates the complex relationship between hydroclimate and volcanic activity in the evolution of lacustrine basins. The Chalco Basin originated as a result of volcanic activity and was infilled in the early stages by mostly volcaniclastic facies and lavas reworked by fluvial and alluvial processes. The thickness of this basal unit is over 200 m at the coring site and our preliminary chronology suggests a minimal age of 367 ka. Initial lacustrine deposition started in the Chalco Basin after this fluvial–alluvial phase and has continued into historic times. Deposition was dominated by alternating diatomaceous, carbonate, and organic-rich facies on scales of 10s of meters. Laminated diatomaceous facies occurred during phases with relatively deep depositional environments. Carbonate deposition marked more alkaline phases. Peat and organic-rich silt were deposited during shallow phases with development of wetlands in the basin.

The preliminary results of the MexiDrill cores show the high potential of the Chalco sequence to provide detailed information on millennial scale variability, the climate during past interglacials, and the relationships among rates of climate change, ecosystem responses, and biodiversity, as well as volcanic and tectonic evolution as the geochronology improves. The cores hold geologic, paleoenvironmental, and paleobiological information that is directly relevant to the >25 million people living in the Basin of Mexico who face challenges related to climate change, volcanic hazards, seismicity, and hydrology. Knowledge of the complex history of past environments can aid in developing policies to mitigate regional consequences of a warming world.

Acknowledgments The MexiDrill Field campaign was funded by ICDP, US National Science Foundation, and UNAM DGAPA-PAPIIT IV100215. M. S. gratefully acknowledges support from the Swiss National Science Foundation grant P300P2 158501.

References

Alaniz-Álvarez, S. A., & Nieto-Samaniego, A. F. (2005). El sistema de fallas Taxco-San Miguel de Allende y la Faja Volcánica Transmexicana, dos fronteras tectónicas del centro de Mexico activas durante el Cenozoico. *Boletín de la Sociedad Geológica Mexicana, 57*(1), 65–82.

An, Z., Colman, S. M., Zhou, W., Li, X., Brown, E. T., Jull, A. J. T., Cai, Y., Huang, Y., Lu, X., Chang, H., Song, Y., Sun, Y., Xu, H., Liu, W., Jin, Z., Liu, X., Cheng, P., Liu, Y., Ai, L., Li, X., Liu, X., Yan, L., Shi, Z., Wang, X., Wu, F., Qiang, X., Dong, J., Lu, F., & Xu, X. (2012). Interplay between the Westerlies and Asian monsoon recorded in Lake Qinghai sediments since 32 ka. *Nature Scientific Reports, 2*, 1–6.

Arce, J. L., Macías, J. L., & Vázquez-Selem, L. (2003). The 10.5 ka Plinian eruption of Nevado de Toluca volcano, Mexico: Stratigraphy and hazard implications. *Geological Society of America Bulletin, 115*, 230–248.

Arce, J. L., Layer, P. W., Lassiter, J. C., Benowitz, J. A., Macias, J. L., & Ramírez-Espinosa, J. (2013a). 40Ar/39Ar dating, geochemistry, and isotopic analyses of the Quaternary Chichinautzin volcanic field, south of Mexico City: Implications for timing, eruption rate, and distribution of volcanism. *Bulletin of Volcanology, 75*, 774.

Arce, J. L., Layer, P. W., Morales-Casique, E., Benowitz, J. A., Rangel, E., & Escolero, O. (2013b). New constraints on the subsurface geology of the Mexico City Basin: The San Lorenzo Tezonco deep well, on the basis of 40Ar/39Ar geochronology and whole-rock chemistry. *Journal of Volcanology and Geothermal Research, 266*, 34–49.

Arce, J. L., Layer, P., Martínez, I., Salinas, J. I., Macías-Romo, M. D. C., Morales-Casique, E., & Lenhardt, N. (2015). Geología and estratigrafía del pozo profundo San Lorenzo Tezonco and de sus alrededores, sur de la Cuenca de Mexico. *Boletín de la Sociedad Geológica Mexicana, 67*(2), 123–143.

Avendaño-Villeda, D. (2017). *Reconstrucción paleolimnológica en el registro del lago de Chalco durante la transición del Estadio Isotópico Marino 6 a 5 (MIS 6 a MIS 5)*, Mexico, Universidad Nacional Autónoma de Mexico, Mexico.

Bhattacharya, T., & Byrne, R. (2016). Late Holocene anthropogenic and climatic influences on the regional vegetation of Mexico's Cuenca Oriental. *Global and Planetary Change, 138*, 56–69.

Bloomfield, K. (1975). A late-quaternary monogenetic volcano field in Central Mexico. *Geologische Rundschau, 64*(1), 476–497.

Bradbury, J. P. (1989). Late Quaternary lacustrine paleoenvironments in cuenca de Mexico. *Quaternary Science Reviews, 8*, 75–100.

Brown, E. T., Werne, J. P., Lozano-García, S., Caballero, M., Ortega-Guerrero, B., Cabral-Cano, E., Valero-Garces, B. L., Schwalb, A., & Arciniega-Ceballos, A. (2012). Scientific drilling in the Basin of Mexico to evaluate climate history, hydrological resources, and seismic and volcanic hazards. *Scientific Drilling, 14*, 72–75.

Brown, E. T., Caballero, M., Fawcett, J. P. T., Lozano-García, S., Ortega, B., Pérez, L., Schwalb, A., Smith, V., Steinman, B. A., Stockhecke, M., Valero-Garcés, B., Watt, S., Wattrus, N. J., Werne, J. P., Wonik, T. H., Myrbo, A. E., Noren, A., O'Grady, R., Schnurrenburger, D., & The MexiDrill Team. (2019). Scientific drilling of Lake Chalco, Basin of Mexico (Mexidrill). *Scientific Drilling, 26*, 1–15. https://doi.org/10.5194/sd-26-1-2019.

Caballero, M., & Ortega-Guerrero, B. (1998). Lake levels since about 40,000 years ago at Lake Chalco, near Mexico City. *Quaternary Research, 50*, 69–79.

Caballero, M., Lozano, S., Ortega, B., Urrutia, J., & Macias, J. L. (1999). Environmental characteristics of Lake Tecocomulco, northern Basin of Mexico, for the last 50,000 years. *Journal of Paleolimnology, 22*, 399–411.

Caballero, M., Lozano-García, S., Ortega-Guerrero, B., & Correa-Metrio, A. (2019). Quantitative estimates of orbital and millennial scale climatic variability in Central Mexico during the last ~40,000 years. *Quaternary Science Reviews, 205*, 62–75.

Cabral-Cano, E., Osmanoglu, B., Dixon, T., Wdowinski, S., DeMets, C., Cigna, F., & Díaz-Molina, O. (2010). Subsidence and fault hazard maps using PSI and permanent GPS networks in Central Mexico. *International Association of Hydrological Sciences, Publication Series, 339*, 255–259.

Campos-Enríquez, J. O., Alatriste-Vilchis, D. R., Huizar-Álvarez, R., Marines-Campos, R., & Alatorre-Zamora, M. A. (2003). Subsurface structure of the Tecocomulco sub-basin (northeastern Mexico Basin), and its relationship to regional tectonics. *Geofísica Internacional, 42*(1), 3–24.

Chen, Ch., McGee, D., Woods, A., Pérez, L., Hatfield, R., Edwards, L. ,Cheng, H., Valero-Garcés, B., Lehmann, S., Stoner, J., Schwalb, A., Tal, I., Seltzer, G., Tapia, P., Abbott, M., Rodbell, D. (2020). U-Th dating of lake sediments: Lessons from the 700 ka sediment record of Lake Junín, Peru. *Quaternary Science Reviews, 244*, https://doi.org/10.1016/j.quascirev.2020.106422.

Colman, S. M., Yu, S.-Y., An, Z., Shen, J., & Henderson, A. C. G. (2007). Late-Cenozoic climate changes in China's western interior: A review of research on Lake Qinghai and comparison with other records. *Quaternary Science Reviews, 26*, 2281–2300.

De Cserna, Z., de la Fuente-Duch, M., Palacios-Nieto, M., Triay, L., Mitre-Salazar, L. M., & Mota-Palomino, R. (1988). Estructura geológica, gravimetría, sismicidad y relaciones neotectónicas regionales de la Cuenca de Mexico: Mexico, D.F., Universidad Nacional Autónoma de Mexico, Instituto de Geología, Boletín 104, 71 p.

Deino, A. L., Dommain, R., Keller, C. B., Potts, R., Behrensmeyer, A. K., Beverly, E. J., King, J., Heil, C. W., Stockhecke, M., Brown, E. T., Moerman, J., de Menocal, P., & Olorgesailie Drilling Project Scientific Team. (2019). Chronostratigraphic model of a high-resolution drill core record of the past million years from the Koora Basin, South Kenya Rift: Overcoming the difficulties of variable sedimentation rate and hiatuses. *Quaternary Science Reviews, 215*, 213–231.

Delgado-Granados, H., & Martín del Pozo, A. L. (1993). Pliocene to Holocene volcanic geology at the junction of Las Cruces, Chichinahutzin and Ajusco ranges southwest of Mexico City. *Geofísica Internacional, 34*, 341–351.

Enciso-De la Vega, S. (1992). Propuesta de nomenclatura estratigráfica para la cuenca de Mexico: Mexico, Universidad Nacional Autónoma de Mexico, Instituto de Geología. *Revista, 10*(1), 26–36.

Ezcurra, E. (1990). The Basin of Mexico. In B. L. Turner (Ed.), *The earth as transformed by human action, global and regional changes in the biosphere over the past 300 years* (pp. 577–588). New York: Cambridge University Press.

Fawcett, P. J., Werne, J. P., Anderson, R. S., Heikoop, J. M., Brown, E. T., Berke, M. A., Smith, S., Goff, F., Donohoo-Hurley, L. L., Cisneros-Dozal, L. M., Schouten, S., Sinninghe Damsté, J. S., Huang, Y., Toney, J., Fessenden, J., Wolde, G. G., Atudorei, V., Geissman, J. W., & Allen, C. D. (2011). Extended Megadroughts in the Southwestern United States during Pleistocene Interglacials. *Nature, 470*, 518–521. https://doi.org/10.1038/nature09839.

Ferrari, L., Orozco-Esquivel, T., Manea, V., & Manea, M. (2012). The dynamic history of the Trans-Mexican Volcanic Belt and the Mexico subduction zone. *Tectonophysics, 522–523*, 122–149.

Fritz, S., Baker, P., Seltzer, G., Ballantyne, A., Tapia, P., Cheng, H., & Edwards, L. (2007). Quaternary glaciation and hydrologic variation in the South American tropics as reconstructed from the Lake Titicaca drilling project. *Quaternary Research, 68*, 410–420.

García-Palomo, A., Carlos-Valerio, V., López-Miguel, C., Galván-García, A., & Concha-Dimas, A. (2006). Landslide inventory map of Guadalupe range, north of the Mexico Basin. *Boletín de la Sociedad Geológica Mexicana, 58*(2), 195–204.

García-Palomo, A., Zamorano, J. J., López-Miguel, C., Galván-García, A., Carlos-Valerio, V., Ortega, R., & Macías, J. L. (2008). El arreglo morfoestructural de la Sierra de Las Cruces, Mexico central. *Revista Mexicana de Ciencias Geológicas, 25*(1), 158–178.

Gierlowski-Kordesch, E., & Kelts, K. (Eds.). (1994). *Global geological record of Lake Basins* (World and regional geology series, 427 pp) (Vol. I. IGCP Project 324). Cambridge University Press.

Gierlowski-Kordesch, E., & Kelts, K. (2001). Lake Basins through space and time. *American Association of Petroleum Geologists Study Geology, 46*, 648 p.

Herrera-Hernández, D. (2011). *Estratigrafía y análisis de facies de los sedimentos lacustres del Cuaternario tardío en la cuenca de Chalco*. Mexico: Universidad Nacional Autónoma de Mexico, Ciudad de Mexico.

Hodell, D., Anselmetti, F., Brenner, M., Ariztegui, D., & the PISDP Science Party. (2006). The Lake Petén Itzá scientific drilling project. *Scientific Drilling, 3*, 25–29.

Jaimes-Viera, C., Martin del Pozzo, A. L., Layer, P. W., Benowitz, J. A., & Nieto-Torres, A. (2018). Timing the evolution of a monogenetic volcanic field: Sierra Chichinautzin, Central Mexico. *Journal of Volcanology and Geothermal Research, 356*, 225–242.

Koeberl, C., Peck, J., King, J., Milkereit, B., Overpeck, J., & Scholz, C. (2005). The ICDP lake Bosumtwi drilling project: A first report. *Scientific Drilling, 1*, 23–27.

Lake Baikal Paleoclimate Project Members. (1992). Initial results of U.S.-Soviet Paleoclimate Study of Lake Baikal. *Eos, Transactions, American Geophysical Union, 73*(43), 457–462.

Litt, T., Anselmetti, F. S., Baumgarten, H., Beer, J., Cagatay, N., Cukur, D., Damci, E., Glombitza, C., Haug, G., Heumann, G., Kallmeyer, J., Kipfer, R., Krastel, S., Kwiecien, O., Meydan, A. F., Orcen, S., Pickarski, N., Randlett, M. E., Schmincke, H.-U., Schubert, C. J., Sturm, M., Sumita, M., Stockhecke, M., Tomonaga, Y., Vigliotti, L., Wonik, T., & the PALEOVAN Scientific Team. (2012). 500,000 years of environmental history in Eastern Anatolia: The PALEOVAN drilling project. *Scientific Drilling, 14*, 18–29.

Lozano-García, M. S., & Ortega-Guerrero, B. (1994). Palynological and magnetic susceptibility records of Chalco Lake, Central Mexico. *Palaeogeography, Palaeoclimatology, Palaeoecology, 109*, 177–191.

Lozano-García, M. S., & Ortega-Guerrero, B. (1998). Late quaternary environmental changes of the central part of the Basin of Mexico; correlation between Texcoco and Chalco Basins. *Review of Paleobotany and Palynology, 99*, 77–93.

Lozano-García, S., Ortega-Guerrero, B., Caballero-Miranda, M., & Urrutia-Fucugauchi, J. (1993). Late Pleistocene and Holocene paleoenvironments of the Chalco lake, Central Mexico. *Quaternary Research, 40*, 332–342.

Lozano-García, S., Ortega, B., Roy, P. D., Beramendi-Orosco, L., & Caballero, M. (2015). Climatic variability in the northern part of the American tropics since the latest MIS 3. *Quaternary Research, 85*(2), 261–272.

Lozano-García, S., Brown, E., Ortega, B., Caballero, M., Werne, J., Fawcett, P. J., Schwalb, A., Valero-Garcés, B., Schnurrenberger, D., O'Grady, R, Stockhecke, M., Steinman, B., Cabral-Cano, E., Caballero, C., Sosa-Nájera, S., Soler, A., Pérez, L., Noren, A., Myrbo, A., Bücker, M., Wattrus, N., Arciniega, A., Wonik, T. H., Watt, S., Kumar, D., Acosta, C., Martínez, I., Cossio, R., Ferland, T., & Vergara-Huerta, F. (2017). Perforación profunda en el lago de Chalco: reporte técnico. *Boletín de la Sociedad Geológica Mexicana, 69*(2), 299–311.

Lugo-Hubp, J. (1984). Geomorfología del Sur de la Cuenca de Mexico, Instituto de Geografía, UNAM, Mexico. *Serie Varia, 1*(8), 1–95.

Lugo-Hubp, J., Mooser, F., Pérez-Vega, A., & Zamorano-Orozco, J. (1994). Geomorfología de la Sierra de Santa Catarina, D.F., Mexico. *Revista Mexicana de Ciencias Geológicas, 11*(1), 43–52.

Macías, J. L., Arce, J. L., García-Tenorio, F., Layer, P. W., Rueda, H., Reyes-Agustín, G., López-Pizaña, F., & Avellán, D. (2012). Geology and geochronology of Tlaloc, Telapón, Iztaccíhuatl and Popocatépetl volcanoes, Sierra Nevada, Central Mexico. In J. J. Aranda-Gómez, G. Tolson, & R. S. Molina-Garza (Eds.), The southern Cordillera and Beyond *Geological Society of America, field guide* (Vol. 25, pp. 163–193).

Martín del Pozzo, A. L. M. (1982). Monogenetic vulcanism in sierra Chichinautzin, Mexico. *Bulletin of Volcanology, 45*(1), 9–24.

Martínez Abarca, R. (2019). *Lago de Chalco: registro sedimentario y estratigráfico de sus etapas formativas*. Tesis de Maestria. UNAM, 128 p.

Martínez-Abarca, R., Ortega-Guerrero, B., Lozano-García, S., Caballero, M., Valero-Garcés, B., McGee, D., … Hodgetts, A. G. E. (2021). Sedimentary stratigraphy of Lake Chalco (Central Mexico) during its formative stages. International Journal of Earth Sciences, 1–21. https://doi.org/10.1007/s00531-020-01964-z

Melles, M., Brigham-Grette, J., Minyuk, P. S., Nowaczyk, N. R., Wennrich, V., DeConto, R. M., Anderson, P. A., Andreev, A. A., Coletti, A., Cook, T. L., Haltia-Hovi, E., Kukkonen, M., Lozhkin, A. V., Rosén, P., Tarasov, P. E., Vogel, H., & Wagner, B. (2012). 2.8 million years of Arctic climate change from Lake El'gygytgyn, NE Russia. *Science, 337*(6092), 315–320.

Metcalfe, S. E., Jones, M. D., Davies, S. J., Noren, A., & MacKenzie, A. (2010). Climate variability over the last two millennia in the North American monsoon region, recorded in laminated lake sediments from Laguna de Juanacatlán, Mexico. *The Holocene, 28*, 1195–1206.

Mosiño-Alemán, P. A., & García, E. (1974). The climate of Mexico. In R. A. H. Bryson & F. K. Hare (Eds.), *Climates of North America* (Vol. 2, pp. 345–405). New York: Elsevier.

Nixon, G. (1989). The geology of Iztaccíhuatl Volcano and adjacent areas of the Sierra Nevada and Valley of Mexico: Geological Society of America Special Paper 219, 58 p.

Ortega-Guerrero, B. (1992). *Paleomagnestismo, magnetoestrtifia y paleoecologia del Cuaternario tardio en el Lago de Chalco, Cuenca de Mexico (Tesis doctoral)*. Universidad Nacional Autónoma de Mexico.

Ortega-Guerrero, B., Lozano García, M., Caballero, M., & Herrera Hernández, D. A. (2015). Historia de la evolución deposicional del lago de Chalco, Mexico, desde el MIS 3. *Boletín de la Sociedad Geológica Mexicana, 67*(2), 185–201.

Ortega-Guerrero, B., Lozano-García, M. S., Herrera-Hernández, D., Caballero, M., Beramendi Orosco, L. E., Bernal, J. P., Torres-Rodríguez, E., & Avendaño-Villeda, D. (2017). Lithostratigraphy and physical properties of lacustrine sediments of the last ca. 150 kyr from Chalco Basin, Central Mexico. *Journal of South American Earth Sciences, 79*, 507–524.

Ortega-Guerrero, B., García, L. C., & Linares-López, C. (2018). Tephrostratigraphy of the late Quaternary record from Lake Chalco, Central Mexico. *Journal of South American Earth Sciences, 81*, 122–140.

Ortiz Zamora, D. D. C., & Ortega Guerrero, M. A. (2007). Origen y evolución de un nuevo lago en la planicie de Chalco: implicaciones de peligro por subsidencia e inundación de áreas urbanas en Valle de Chalco (Estado de Mexico) y Tláhuac (Distrito Federal). *Investigaciones geográficas, 64*, 26–42.

Oviedo de León, A. (1970). El Conglomerado Texcoco y el posible origen de la Cuenca de Mexico. *Revista del Instituto Mexicano del Petróleo, 2*, 5–20.

Pérez-Cruz, G. A. (1988). Estudio sismológico de reflexión del subsuelo de la Ciudad de Mexico: Mexico, D.F., Universidad Nacional Autónoma de Mexico, Tesis de Maestría, División de Estudios de Posgrado de la Facultad de Ingeniería, 83 p.

Peterson, L. C., Haug, G. H., Hughen, K. A., & Rohl, U. (2000). Rapid changes in the hydrologic cycle of the tropical Atlantic during the last glacial. *Science, 290*, 1947–1951.

Pi, T., Lozano-García, S., Caballero-Miranda, M., Ortega-Guerrero, B., & Roy, P. (2010). Discovery and characterization of a struvite layer in the Chalco paleolake, Mexico. *Revista Mexicana de Ciencias Geológicas, 27*(3), 573–580.

Pueyo, J. J., Sáez, A., Giralt, S., Valero-Garcés, B. L., Moreno, A., Bao, R., Schwalb, A., Herrera, C., Klosowska, B., & Taberner, C. (2011). Carbonate and organic matter sedimentation and isotopic signatures in Lake Chungará, Chilean Altiplano, during the last 12.3 kyr. *Palaeogeography, Palaeoclimatology, Palaeoecology, 307*, 339–355.

Ruiz-Angulo, A., & López-Espinoza, E. D. (2015). Estimación de la respuesta térmica de la cuenca lacustre del Valle de Mexico en el siglo XVI: un experimento numérico. *Boletín de la Sociedad Geológica Mexicana, 67*(2), 215–225.

Russell, J. M., Bijaksana, S., Vogel, H., Melles, M., Kallmeyer, J., Ariztegui, D., Crowe, S. A., Fajar, S. J., Hafidz, A., Haffner, D., Hasberg, A. K. M., Ivory, S. J., Kelly, C., King, J. W., Kirana, K. H., Morlock, M. A., Noren, A., O'Grady, R., & Ordonez, L. (2016). The Towuti Drilling Project: Paleoenvironments, Biological Evolution, And Geomicrobiology Of A Tropical Pacific Lake. *Scientific Drilling, 21*, 29–40.

Schnurrenberger, D., Russell, J., & Kelts, K. (2003). Classification of lacustrine sediments based on sedimentary components. *Journal of Paleolimnology, 29*, 141–154.

Scholz, C. A., Johnson, T. C., Cohen, A. S., King, J. W., Peck, J. A., Overpeck, J. T., Talbot, M. R., Brown, E. T., Kalindekafe, L., Amoako, P. Y. O., Lyons, R. P., Shanahan, T. M., Castañeda, I. S., Heil, C. W., Forman, S. L., McHargue, L. R., Beuning, K. R., Gomez, J., & Pierson, J. (2007). East African megadroughts between 135–75 kyr ago and implications for early human history. *Proceedings of the National Academy of Sciences, 104*, 16416–16421.

Schuster, M., Duringer, P., Ghienne, J.-F., Roquin, C., Sepulchre, P., Moussa, A., Lebatard, A.-E., Mackaye, H. T., Likius, A., Vignaud, P., & Brunet, M. (2009). Chad Basin: Paleoenvironments of the Sahara since the late Miocene. *Comptes Rendus Geosciences, 341*, 612–620.

Siebe, C. (2000). Age and archaeological implications of Xitle volcano, southwestern Basin of Mexico City. *Journal of Volcanology and Geothermal Research, 104*(1), 45–64.

Siebe, C., Macias, J. L., Abrams, M., Rodriguez, S., Castro, R., & Delgado, H. (1995). Quaternary explosive volcanism and pyroclastic deposits in East Central Mexico: Implications for future hazards. In *Guidebook of geological excursions: In conjunction with the annual meeting of the Geological Society of America, New Orleans, Louisiana, November 6–9, 1995* (pp. 1–48). Baton Rouge: Louisiana State University. Basin Research Institute. Center for Coastal Energy & Environmental Resources.

Siebe, C., Macías, J., Abrams, M., Rodríguez, S., & Castro, R. (1997). *Catastrophic prehistoric eruptions at Popocatépetl and Quaternary explosive volcanismin the Serdán-Oriental basin, east-central Mexico*. Pre-meeting excursion fieldtrip guidebook No 4, January 12–18: Puerto Vallarta, Mexico, International Association of Volcanology and Chemistry of the Earth's Interior (IAVCEI) General Assembly (88 pp.).

Siebe, C., Schaaf, P., & Urrutia-Fucugauchi, J. (1999). Mammoth bones embedded in a late Pleistocene lahar from Popocatépetl volcano, near Tocuila, Central Mexico. *Geological Society of America Bulletin, 111*, 1550–1562.

Siebe, C., Rodríguez-Lara, V., Schaaf, P., & Abrams, M. (2004). Geochemistry, Sr-Nd isotope composition, and tectonic setting of Holocene Pelado, Guespalapa and Chichinautzin scoria cones, south of Mexico City. *Journal of Volcanology and Geothermal Research, 130*, 197–226.

Siebe, C., Arana-Salinas, L., & Abrams, M. (2005). Geology and radiocarbon ages of Tláloc, Tlacotenco, Cuauhtzin, Hijo del Cuauhtzin, Teuhtli, and Ocusacayo monogenetic volcanoes in the central part of the Sierra Chichinautzin, Mexico. *Journal of Volcanology and Geothermal Research, 141*(3), 225–243.

Siebe, C., Salinas, S., Arana-Salinas, L., Macías, J. L., Gardner, J., y Bonasia, R. (2017). The~ 23,500 y 14C BP White Pumice Plinian eruption and associated debris avalanche and Tochimilco lava flow of Popocatépetl volcano, México. *Journal of Volcanology and Geothermal Research, 333*, 66–95.

Sosa-Ceballos, G., Gardner, J. E., Siebe, C., & Macías, J. L. (2012). A caldera-forming eruption~ 14,100 14 Cyr BP at Popocatepetl volcano, Mexico: Insights from eruption dynamics and magma mixing. *Journal of Volcanology and Geothermal Research, 213*, 27–40.

Stein, M., Ben-Avraham, Z., Goldstein, S., Agnon, A., Ariztegui, D., Brauer, A., Haug, G., Ito, E., & Yasuda, Y. (2011). Deep drilling at the dead sea. *Scientific Drilling, 11*, 46–47.

Stockhecke, M., Kwiecien, O., Vigliotti, L., Anselmetti, F. S., Beer, J., Namik Çağatay, M., Channell, J. E. T., Kipfer, R., Lachner, J., Litt, T., Pickarski, N., & Sturm, M. (2014). Chronostratigraphy of the 600,000 year old continental record of Lake Van (Turkey). *Quaternary Science Reviews, 104*, 8–17.

Torres-Rodríguez, E., Lozano-García, S., Roy, P., Ortega, B., Beramendi-Orosco, L., Correa-Metrio, A., & Caballero, M. (2015). Last glacial droughts and fire regimes in the central Mexican highlands. *Journal of Quaternary Science, 30*, 88–99.

Torres-Rodríguez, E., Lozano-García, S., Caballero-Miranda, M., Ortega-Guerrero, B., Sosa-Nájera, S. and Debajyoti-Roy, P. (2018). Pollen and non-pollen palynomorphs of Lake Chalco as indicators of paleolimnological changes in high-elevation tropical central Mexico since MIS 5. *Journal of Quaternary Science, 33*(8), 945–957.

Vazquez-Selem, L., & Heine, K. (2011). Late quaternary glaciation in Mexico. In J. E. Ehlers, P. L. Gibbard, & P. D. Hughes (Eds.), *Quaternary glaciations-extent and chronology: A closer look* (Vol. 15, pp. 849–861). Amsterdam: Elsevier.

Wagner, B., Wilke, T., Krastel, S., Zanchetta, G., Sulpizio, R., Reicherter, K., Leng, M. J., Grazhdani, A., Trajanovski, S., Levkov, Z., Reed, J., & Wonik, T. (2014). More than one million years of history in Lake Ohrid Cores. *Eos, Transactions American Geophysical Union, 95*(3), 25–26.

White, S. E. (1962). Late Pleistocene glacial sequence for the west side of Iztaccíhuatl, Mexico. *Geological Society of America Bulletin, 73*, 935–958.

White, S. E. (1987). Quaternary glacial stratigraphy and chronology of Mexico. *Quaternary Science Reviews, 5*(1–4), 201–206.

Zolitschka, B., Anselmetti, F., Ariztegui, D., Corbella, H., Francus, P., Lücke, A., Maidana, N., Ohlendorf, C., Schäbitz, F., & Wastegard, S. (2013). Environment and climate of the last 51,000 years—New insights from the Potrok Aike maar lake Sediment Archive Drilling Project (PASADO). *Quaternary Science Reviews, 71*, 1–12.